ON THE INTERLAMINAR SHEAR STRESS RESPONSE OF LAYERED COMPOSITE MATERIALS

Khalil M. Elawadly
Mathematical Engineering Physics Department, Faculty of Engineering,
Alexandria University, Alexandria, Egypt.

ABSTRACT

An analytical and experimental investigation has been performed to study the interlaminar shear response of laminated composite material. The main objective of this study is to determine the effect of the stacking sequences and the thickness of the layers on the interlaminar shear strength of E-glass/epoxy laminated composite tubular struts which will be used in superconducting magnetic energy storage. The experimental results showed that the first ply failure always happens at the middle section of the sample and the maximum interlaminar shear stress has its maximum value along the neutral axis. The absence of plies perpendicular to the $\pm 10^{o}$ direction are favorable for a good stress distribution. On the other hand these plies are very important to prevent the brooming under compression loads. The results also showed that the stress distribution, due to less thick and more $\pm 10^{o}$ layers were better and gave a higher interlaminar shear strength. The interfaces between the 84^{o} layer and $\pm 10^{o}$ layer are the most probable locations to start interlaminar shear failure, that is because of the large mismatch in engineering properties between these layers. The experimental results and the corresponding analytical calculations are in good agreement.

Keywords: Composite Materials, Finite Element, E-glass/Epoxy, Failure Mechanisms, Laminates, Interlaminar Shear Stress.

INTRODUCTION

Classical laminate analysis, based on the Kirchhoff hypothesis ignores shear deformations of the layers. However, the importance of these deformations has been well established by Whitney [1] and Pagano [2] in bending problems. The behavior of laminated composites under generalized plane stress is strongly influenced by the presence of the so-called interlaminar shear stresses, that is, shear stresses distributed on the faces of the laminate layers. The interlaminar shear strength may be defined as the resistance of a layered composite to internal forces that tend to induce relative parallel motion to and between the layers [3].

Interlaminar shear strength (ILS) is not an easy measurable mechanical property of a filamentary composite. The large number of ILS test procedures indicates uncertainty about the definition of the property [4]. Furthermore, no existing test procedure for layered composites provides a uniform interlaminar shear stress over a sizable region in the test section of the specimen. Stress concentration builds up at the boundaries of the shear stress field. For multi-directional fibrous composites, the failure process reveals interlaminar shear stress as the most critical stress causing laminate failure. When generalized plane stresses are applied to a laminate, the different layers tend to slide over one another because of the differences in their elastic constants. Since the layers are elastically connected through their faces, relative shear stresses are developed on the faces of each layer. For multi-directional fibrous composites, the failure process reveals interlaminar shear stress as the most critical stress causing laminate failure.

It is found that the laminate ply stacking sequence and the ply fiber orientations greatly influence the onset and growth of free-edge delamination. Bjeletich et al.[5] have shown in their experiment that the uniaxial tensile strength of the graphite/epoxy with fiber orientation $[\pm 45 \pm /0°/90°]_s$ was much smaller than

that of fiber orientation $[0°/90°/\pm45°]_s$. A free-edge stress analysis based on ply elasticity revealed that large interlaminar tensile stresses act along the free edges of a coupon of fiber orientation $[\pm45°/0°/90°]_s$, while compressive interlaminar stresses of comparable magnitude are induced along the free edge of the $[0°/90°/\pm45°]_s$ coupon. Hence, $[\pm45°/0°/90°]_s$ had developed free-edge delamination, while $[0°/90°/\pm45°]_s$ did not develop such delamination.

Actually, ply stacking sequence and ply orientation are not the only lamination variables that affect the free-edge delamination behavior. Rodini et al.[6] showed that the free-edge delamination also depends on the ply thickness. For example, the critical laminate tensile strain at the onset of free-edge lamination in the graphite/epoxy $[\pm45°_n/0°_n/90°_n]_s$ laminate family varies roughly with the inverse value of $\sqrt{n}$. A more systematic study on the ply-thickness effects on the matrix cracking in general have been reported by Crossman et al.[7].

Jen et al [8] developed mathematical model to study the interlaminar edge stresses and singularities in a notched composite laminate and to predict the onset of delamination. They stated that the location of delamination and matrix cracking coincidences with the interfaces of the largest interlaminar shear and normal stresses predicted by their model. Joo and Sun [9] studied the interlaminar shear stresses in balanced and symmetric laminates with free edges and the failure due to these stresses. It was shown that the average interlaminar shear stress near the free edge is linearly related to the mismatch of the extension-shear coupling of the top and bottom sublaminates separated by the interface of interest. Herakovich [10] showed that there is a fundamental relationship between delamination and the mismatch of elastic properties between the adjacent layers of laminated composites. However, no equation describing this relationship has been given. In this study the factors that affect the interlaminar shear stress will be investigated using both finite element analysis and experimental test.

THE SHORT-BEAM-SHEAR TEST

The short-beam-shear test [11] involves a three-point flexure specimen with the span-to-thickness ratio chosen to produce interlaminar shear failure. This test method is popular for seeking interlaminar shear performance of composites because of its simplicity and inexpensive nature.This method is an ASTM standard test method registered D-2344-84 [12]. The shear stress distribution along the thickness of an isotropic specimen is a parabolic function that reaches a maximum value at the center of the thickness of the sample and is zero at both faces. This test also suffers from stress concentration near the applied load and the reaction points at the supports which prevails highly shear stress distribution skewed close to the load and the supports. For this reason our results will be calculated at a location far from these points to avoid this problem. The length to thickness ratio is very important because an improper ratio may induce failure due to combined shear, tensile or compression stresses. Inspection of the failure mode should show a shear failure parallel to the beam axis. In this study the length to thickness ratio used is approximately five.

The interlaminar shear stress (τ_i) is determined from the equation:

$$\tau = \frac{3\,P}{4bh}$$

where: (P) is the applied force, (b) is the width and (h) is the thickness of the sample.

TEST PROCEDURE.c.:

The specimen were tested under a load frame equipped with a hydraulic power supply. The general test conditions are: the span of the specimen is equal to five times the thickness (31.75 mm.), the lengseven times the th(44.45 mm.), the arc of the specimen is 12°, the loading nose radius is 3.175 mm. (1/8 inch). The specimen is supported by two reaction noses with an arc of radius 1.5875 mm. (1/16 inch) at the contact area., the cross head speed is 1.27 mm/minute, and the reaction noses are free to move sidewards The reaction noses may roll sidewards due to the two pins. The loading nose, with an arc of 1/8 inch moves in the direction of the applied load at constant speed.

The arc sample cut out of tube has an inner radius of 26.95 mm, the thickness is 6.35 mm and the arc angle is 12°. The tubes are E-glass reinforced epoxy manufactured by filament winding by Addax Inc., Lincoln Nebraska. The matrix material is epoxy, named Addax1. The fiber volume is 58% (±1%) and the void

content is 2% maximum.

FINITE ELEMENT MODEL

The analysis was performed using the finite element code ANSYS version 5.2 [13]. This code incorporates a three-dimensional composite layered that allows the calculation of the stress components in three directions. The model chosen for the analysis is a part of cylindrical tube with inner and outer diameters of 53.9 mm and 66.6 mm respectively. The number of element was 56 elements, and the number of nodes was 322 nodes. The tubes are made of E-glass reinforced epoxy laminated composite. The material properties for this material are presented in Table (1). Five different winding pattern of samples called " A, B, C, D, and E" are used in this study. The winding pattern " fiber orientation" of the samples are [84°, $\pm 10°_2$,84°, $\pm 10°_2$,84°], [84°, $\pm 10°_3$,84°, $\pm 10°_3$,84°] , [84°, $\pm 10°_4$,84°, $\pm 10°_4$,84°], $[\pm 10°]_8$, and $[\pm 10°_3, \pm 84°]_3$ respectively.

Table 1. Material properties of E-glass/epoxy.

Material properties		
Fiber volume fraction	=	58% ± 1%
Void content	=	2% max.
Young modulus		
E_x	=	39.3 GPa
E_y	=	9.653 GPa
E_z	=	9.653 GPa
Shear modulus		
G_{xy}	=	2.206 GPa
G_{xz}	=	2.206 GPa
G_{yz}	=	0.896 GPa
Poison's ratio	=	0.25

The interlaminar shear specimen used in this analysis has arc angle of 12°, length 44.5 mm and span length 31.75 mm. The boundary conditions are chosen such that the specimen has the ability to expand without restriction, i.e. avoiding the existence of stress concentration as a result of the poison's ratio effect. For stress analysis, the region of interest was subdivided into a number of elements with a very dense and uniform mesh.

Tsai and Wu [14] failure criteria will be used in this analysis to investigate the results and to check the onset of failure. They assumed a failure surface in stress space of the form,

$$f(\sigma) = F_i\,\sigma_i + F_{ij}\,\sigma_i\,\sigma_j \quad (i, j = 1,2,3,4,5,6) \qquad (1)$$

which can be expanded as

$$f = \left(\frac{1}{X_t} + \frac{1}{X_c}\right)\sigma_1 + \left(\frac{1}{Y_t} + \frac{1}{Y_c}\right)\sigma_1 + \left(\frac{1}{Z_t} + \frac{1}{Z_c}\right)\sigma_3$$

$$+ \frac{(\sigma_1)^2}{X_t X_c}\frac{(\sigma_2)^2}{Y_t Y_c}\frac{(\sigma_3)^2}{Z_t Z_c} + \frac{(\tau_{12})^2}{(S_{12})^2}\frac{(\tau_{23})^2}{(S_{23})}\frac{(\tau_{13})^2}{(S_{13})}$$

$$+ \frac{C_{12}\sigma_1\sigma_2}{\sqrt{X_t X_c Y_t Y_c}} + \frac{C_{23}\sigma_2\sigma_3}{\sqrt{X_t X_c Z_t Z_c}} + \frac{C_{13}\sigma_1\sigma_3}{\sqrt{X_t X_c Z_t Z_c}}$$

where

f: is the Tsai-Wu failure criterion value,

$\sigma_1, \sigma_2, \sigma_3, \tau_{12}, \tau_{23}, \tau_{13}$ are the computed layer component normal and shear stresses,

$X_t, Y_t, Z_t, X_c, Y_c, Z_c$ are the tensile and compressive strength along 1,2 and 3-axis,

S_{12}, S_{23}, S_{13} are the shear strength components,

C_{12}, C_{23}, C_{13} are the coupling coefficients for Tsai-Wu. In the absence of the biaxial data, Tsai and Hahn [15] have proposed taking the coupling coefficient (C's) equal to -1 .

The compressive strengths X_c, Y_c, and Z_c are taken as positive numbers.

In each interface, the interlaminar failure criterion used in this study is given by [16]:

$$\left(\frac{\sigma_3}{Z_i}\right)^2 + \left(\frac{\tau_{23}}{S_i}\right)^2 + \left(\frac{\tau_{31}}{S_i}\right)^2 = 1 \qquad (2)$$

where σ_3, τ_{32}, τ_{31} are the average interlaminar stresses over critical distance of 2t (where t is ply thickness), Z_i is the peel strength. and S_i is the interlaminar shear strength.

EXPERIMENTAL RESULTS

The sample test set up is shown in Figure (1). The samples have been tested in both sides to investigate the interlaminar shear strength. The reversed test (upside down) will be referred to as "inverted" ILS. The upside down test results show slightly higher or lower interlaminar shear strength than that obtained for the normal case. The results show that the applied load increases linearly with the displacement until reaching the maximum value and then drop suddenly (sharp peak) indicating that the first ply failure occurs in the sample. After this peak the load begins to increase again to a second peak ,which does not exceed the first one, and drops again which means that another failure happens. Two samples of each winding pattern are stopped after the first peak to investigate the first ply failure and also the failure mode. The investigation shows that the first ply failure always occurs in the middle section of the sample, which agree well with the theory. All curves have a very sharp peak in the load displacement curves followed by load drop. This results agree well with those obtained by Daniels et al [17] for graphite fiber composite. Discrete shear failures are accompanied by the load drop. This failure mode is observed for all the tested samples in this study which indicate that the samples failed under interlaminar shear.

Samples of winding pattern D which have a fiber orientation $[\pm 10°_3, \pm 84°]_3$ show a large drop of load after the first peak followed by a very low second peak. Samples of winding pattern A, B, C and E have a higher second peak compared to those observed for samples of winding pattern D. It is also observed that the ILS inverted test for sample D gives a small drop at the beginning of the loading. After this drop the load continues to increase again with the same slope to its maximum. The $\pm 84°$ layer at the outside of the sample probably fails and causes this almost imperceptible load drop. The investigation of the failure mechanisms of samples of winding pattern D show that the matrix of the $\pm 84°$ layer failed due to interlaminar transverse shear stress. The next interface failure is also at the boundary of $\pm 84°$ layer and $\pm 10°$ layer. The matrix of the $\pm 84°$ layer also failed here. There is no other failure in between these two failure interfaces. For sample, in the C and E modes the failure interface is located between a -10° layer and a +10° layer. Figure (2) shows a microscopic photographs of the crack surface of the specimen.

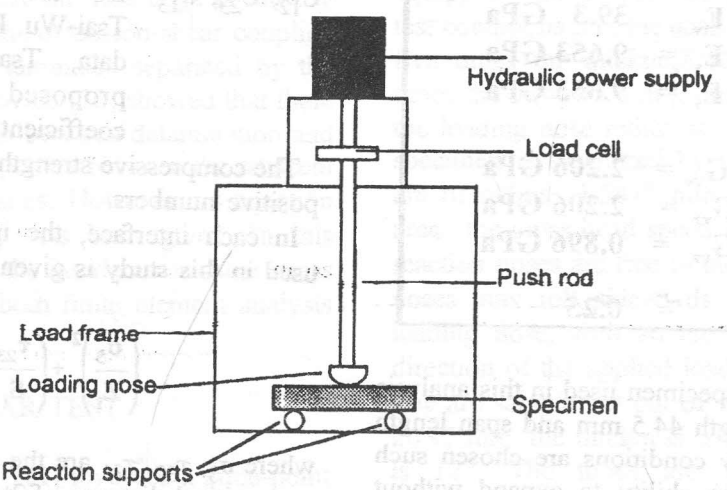

Figure 1. Test set up configuration.

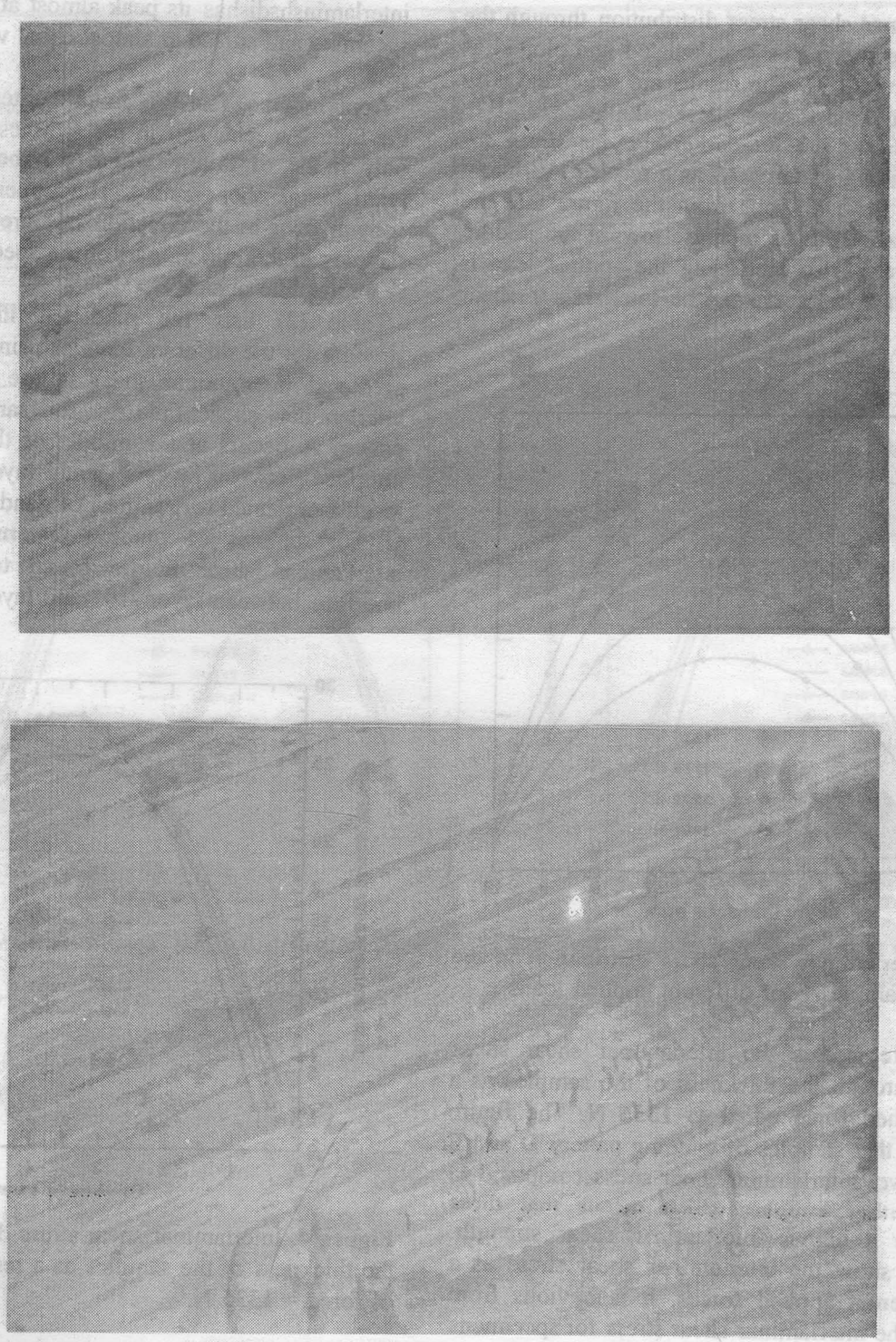

Figure 2. Microscopic photograph of the crack surface of the specimens.

FINITE ELEMENT RESULTS

The interlaminar shear stress distribution through the thickness of the specimens is calculated and plotted as shown in Figures (3-7). The results are generated with four different applied loads to each sample.

Figure (3) shows the interlaminar shear stress for samples of winding pattern A as a result to different applied forces. It is obvious from the figure that the interlaminar shear stresses increase toward the middle of the specimen. Also increasing the applied load is associated with an increase of the interlaminar shear stress.

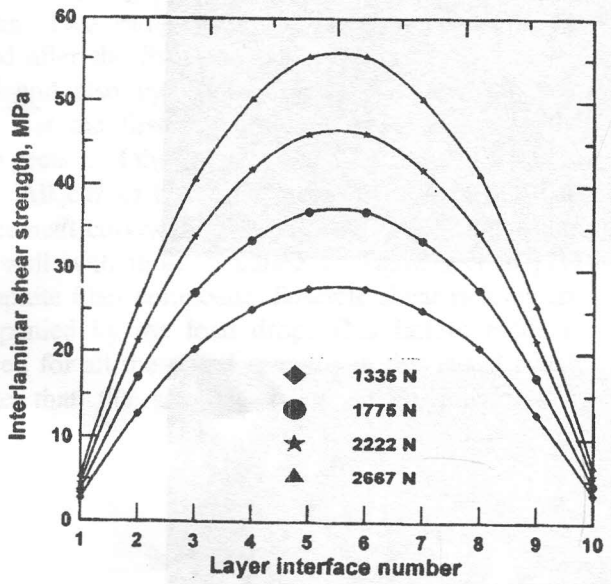

Figure 3. Interlaminar shear stress distribution at the interfaces of sample A for different applied loads.

Figure (4) represents the interlaminar shear stress distribution through the thickness of the samples as a result of applied force equal to 1335 N. The figure shows clearly that samples of winding pattern D and E result in a lower interlaminar shear stress compared to that of the other samples which means that these samples have a higher interlaminar shear strength. Figures (5-7) show the interlaminar shear stress as a result of different applied forces. It is obvious from figure 5 that the interlaminar shear stress for specimens of winding pattern E is less than those obtained for the specimens of winding pattern A, B, C, and even D. Figure 8 represents the interlaminar shear stress distribution along the length of specimen of winding pattern C. It is obvious from that figure that the interlaminshsdishas its peak almost at the middleof the specimen and spread at almost equal values around that peak.

Applying the Tsai-Wu failure criteria to investigate the failure mechanism in the samples indicate that the only mode of failure which can be obtained is the interlaminar shear stress. The upper laminate which contain fiber in the direction 84° are failed for all the samples in the middle part of the specimens as a result to matrix microcrack.

Table (2) lists the predicted interlaminar shear strength for the different samples using equation 2. The predicted interlaminar shear failure indicate that the interlaminar shear failure for sample of winding pattern A occurs at the middle of the samples at the interface between layer 84° and layer 10°. The same result is obtained for samples of winding pattern B and C. For samples of winding pattern D and "E" the interlaminar shear failure found to occur at the interface between layer -10° and layer +10° .

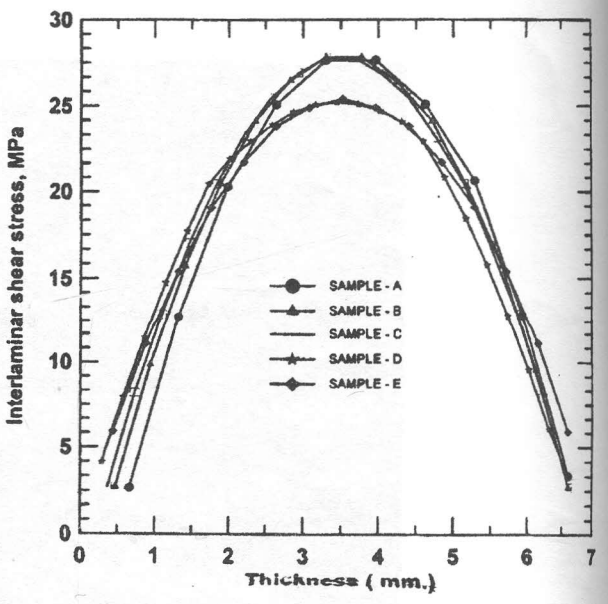

Figure 4. Interlaminar shear stress distribution through the thickness of the samples as a results of force = 1335 N.

Table 2. Experiment predicted interlaminar shear strength.

Sample winding pattern	Interlaminar shear strength [MPa]	Interlaminar shear strength [MPa] "Inverted ILS test"	Predicted Interlaminar shear strength [MPa]
A	34.20	33.85	32.36
B	31.23	29.65	31.66
C	37.92	38.61	36.30
D	41.37	42.75	40.40
E	44.80	42.06	43.12

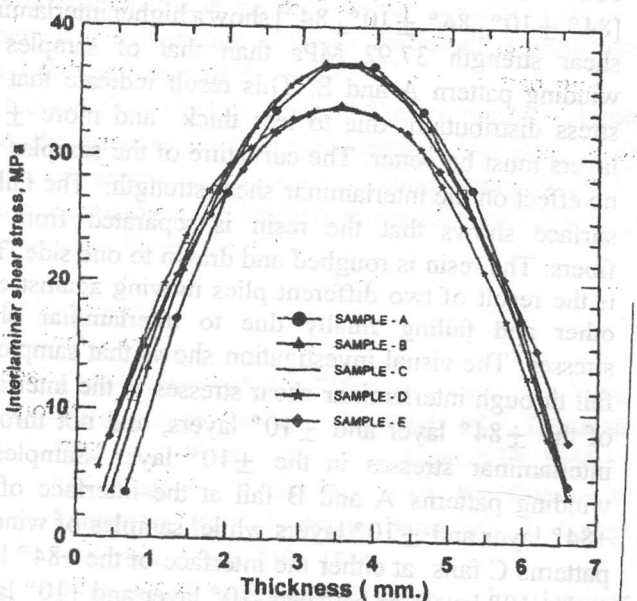

Figure 5. Interlaminar shear stress distribution through the thickness of the samples as a result of force = 1775 N.

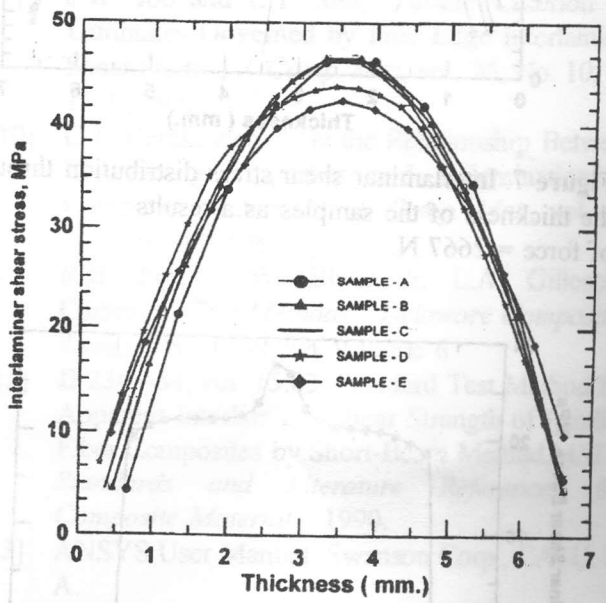

Figure 6. Interlaminar shear stress distribution through the thickness of the samples as a result of force = 2222 N.

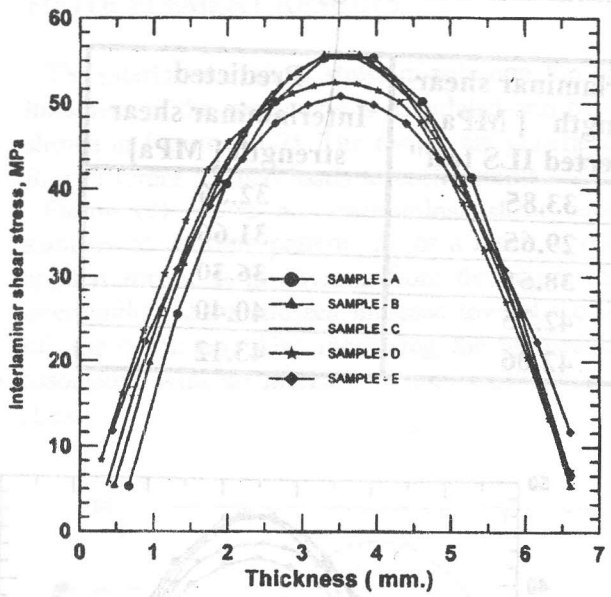

Figure 7. Interlaminar shear stress distribution through the thickness of the samples as a results of force = 2667 N.

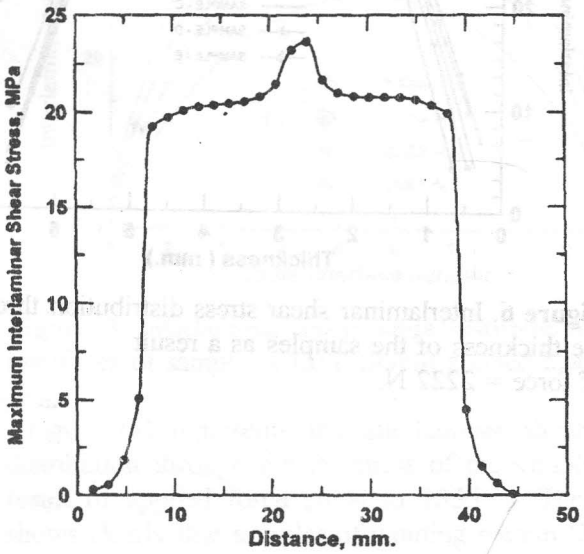

Figure 8. Interlaminar shear stress distribution along the length of specimen of winding pattern C.

DISCUSSION

The first ply failure occur always in the middle section (at the neutral axis) of the sample. Maximum interlaminar shear stress has its maximum along the neutral axis. The visual inspection shows that the failure occurs through the resin or at the interface of resin and fiber and that fibers do not fail.

Samples of winding pattern E, $[\pm 10^{o}]_{8}$, have the highest interlaminar shear strength: 44.82 MPa, which indicate that the absence of plies perpendicular to the $\pm 10°$ layers are favorable for a good stress distribution. Samples of winding patterns A, B, C and D have 84° layer or $\pm 84°$layers respectively in their wind up. The large difference in angle between these layers and the $\pm 10°$ layers creates high stress concentrations as a result of the mismatch in the material properties when these layers move against each other. Samples of winding pattern C $[84°, \pm 10°_{4}, 84°, \pm 10°_{4}, 84°]$ show a higher interlaminar shear strength 37.92 MPa than that of samples of winding pattern A and B. This result indicate that the stress distribution, due to less thick and more $\pm 10^{o}$ layers must be better. The curvature of the samples has no effect on the interlaminar shear strength. The failure surface shows that the resin is separated from the fibers. The resin is roughed and drawn to one side. This is the result of two different plies moving against each other and failing finally due to interlaminar shear stresses. The visual investigation shows that samples D fail through interlaminar shear stresses at the interfaces of the $\pm 84°$ layer and $\pm 10°$ layers, and not through interlaminar stresses in the $\pm 10°$ layer. Samples of winding patterns A and B fail at the interface of the +84° layer and $\pm 10°$ layers while, samples of winding patterns C fails at either the interface of the +84° layer and $\pm 10°$ layers or between -10° layer and +10° layer. This explains the higher interlaminar shear strength obtained for samples of winding patterns C than those for samples of winding patterns A and B. Samples of winding patterns E can only fail at the interface of $\pm 10°$ layers or between an -10° layer and an +10° layer.

CONCLUSIONS

From the previous results we can conclude that the interfaces between the +84° (or $\pm 84°$) layer and the $\pm 10°$ layers are the most probable locations to start interlaminar shear failure, because of the large mismatch in the engineering properties between these layers.

The finite element results agree well with the experiment in spite of the small differences in the interlaminar shear strength. The predicted interlaminar shear strength from the finite element model showed high agreement with the experimental measurement of stress in the laboratory. The difference between the finite element predicted stresses and the measured stresses was found to vary from 1.3 to 5.3 % .

The fundamental reason for the presence of interlaminar shear stresses in laminated composite is the existence of a mismatch in engineering properties between layers and also the thickness of these layers. The results show that the thickness of the layers play an important role in the interlaminar shear strength and there is a conjunction between the stacking sequences and the thickness of the layers..

Neither the effect of ratio of fiber to matrix volume, nor the effect of voids is considered in this work. Both have an impact on interlaminar shear strength, as the matrix is perhaps the limiting factor of shear stresses in composites laminates.

REFERENCES

[1] J.M. Whitney, "The Effect of Transverse Shear Deformation on the Bending of Laminate Plates", *J. Comp. Mat.*, vol. 3, pp. 534, 1969.

[2] N.J. Pagano, "Exact Solutions for Composite Laminates in Cylindrical Bending", *J. Comp. Mat.*, vol. 3, pp. 396, 1969.

[3] H. Becke, "Problems of Cryogenic Interlaminar Shear Strength Testing". Advances in Cryogenic Engineering (Materials), vol. 36, p.827, 1992

[4] D.W. Wilson, "An Overview of Test Methods Used for Shear Characterization of Advanced Composite Materials", *Advances in Cryogenic Engineering*, (Materials), vol. 36, p.793, 1992

[5] S.P. Bjeletich, F.W. Crossman and W.J. Warren "The Influence of Stacking Sequence on Failure Modes in Quasi-Isotropic Graphite/Epoxy Laminates", *In : Failure Modes of Composites-IV,* Cornie J. R. and Crossman F. W., ed., American Institute of Mining, Metallurgical and Petrolium Engineering, New York, pp. 118, 1979.

[6] B.T. Rodini and JH.R. Eisenmann, "An Analytical and Experimental Investigation of Edge Delamination in Composite Laminates", *In : Fibrous Composites in Structural Design*, Lenoe E. M. and Burke J. J., Plenum Press, New York, pp. 441, 1978.

[7] F.W. Crossman and A.S.D. Wang, "The Dependence of Transverse Cracking and Delamination on Ply Thickness in Graphite Epoxy Laminates ", *In : Damage in Composite Materials, Reifsnider K. L., ed., ASTM-STP-775*, pp. 118, 1982.

[8] M. Jen, Y.S. Kau and J.M. Hsu, "Initiation and Propagation of Delamination in a Centrally Notched Composite Laminates", *J. Comp. Mat.*, vol. 27, No. 3, pp. 272, 1993.

[9] J.W. Joo and C.T. Sun, "Failure Criterion for Laminates Governed by Free Edge Interlaminar Shear Stress", *J. Comp. Mat*, vol. 26, No. 10, pp. 1510, 1992.

[10] C.T. Herakovich, " On the Relationship Between Engineering Properties and Delamination of Composite Materials"', *J. Comp. Mat.*, vol. 15, pp. 336-348, 1981.

[11] R.B. Pipes, J.W. Blake Jr, L.A. Gillespie, Carlsson, *"Test Methods", Delaware Composites Design Encyclopedia*, Volume 6

[12] D 2344-84, vol. 15.03, Standard Test Method for Apparent Interlaminar Shear Strength of Parallel Fiber Composites by Short-Beam Method, *ASTM Standards and Literature References for Composite Materials,* 1990.

[13] ANSYS User Manual, Swanson Corp., CA, U. S. A.

[14] S.W. Tsai and E.M. Wu, "A General Theory of Strength for Anisotropic Materials", *J. Comp. Mat.*, vol. 5, pp. 58-80, 1971.

[15] S.W. Tsai and H.T. Hahn, "Introduction to Composite Materials", *Technomic, West Port, CT*, 1980.

[16] R.B. Zhou and C.T. Sun, "Failure Analysis of Composite Laminates With Free Edge", *J. Composite Technology & Research*, vol. 12, pp. 91-97, 1990.

[17] B.K. Daniels, N.K. Harakas, R.C. Jackson, "Short Beam Shear Tests of Graphite Fibers Composites", *Fibre Science and Technology*, vol. 3 , pp.187, 1971.